

2-2000

# Curvature Energy of a Focal Conic Domain with Arbitrary Eccentricity

Maurice Kleman

*Université de Paris*

Oleg Lavrentovich

*Kent State University*, [olavrent@kent.edu](mailto:olavrent@kent.edu)

Follow this and additional works at: <http://digitalcommons.kent.edu/cpipubs>

 Part of the [Physics Commons](#)

---

## Recommended Citation

Kleman, Maurice and Lavrentovich, Oleg (2000). Curvature Energy of a Focal Conic Domain with Arbitrary Eccentricity. *Physical Review E* 61(2), 1574-1578. doi: 10.1103/PhysRevE.61.1574 Retrieved from <http://digitalcommons.kent.edu/cpipubs/80>

This Article is brought to you for free and open access by the Department of Chemical Physics at Digital Commons @ Kent State University Libraries. It has been accepted for inclusion in Chemical Physics Publications by an authorized administrator of Digital Commons @ Kent State University Libraries. For more information, please contact [earicha1@kent.edu](mailto:earicha1@kent.edu), [tk@kent.edu](mailto:tk@kent.edu).

## Curvature energy of a focal conic domain with arbitrary eccentricity

Maurice Kleman<sup>1</sup> and Oleg D. Lavrentovich<sup>2</sup>

<sup>1</sup>*Laboratoire de Minéralogie-Cristallographie, UMR 7590, Université de Paris-VI and Université de Paris-VII, Case 115, 4 place Jussieu, 75252 Paris Cédex 05, France*

<sup>2</sup>*Chemical Physics Interdisciplinary Program and Liquid Crystal Institute, Kent State University, Kent, Ohio 44242*  
(Received 21 June 1999)

The most frequently observed focal conic domains (FCD's) in lamellar phases are those based on confocal pairs of ellipse and hyperbola. Experimentally, the eccentricity of the ellipse takes a broad range of values  $0 \leq e < 1$ . We present an analytical expression for the curvature energy of a FCD that is valid in the entire range  $0 \leq e < 1$ . Generally, the curvature energy of an *isolated* FCD reaches a minimum only at  $e \rightarrow 1$  (under the constraint of a fixed major semiaxis of the ellipse); exceptions include situations with large saddle-splay elastic constant and small domains where the applicability of the elastic theory is limited. In realistic cases, a value of eccentricity smaller than 1 is stabilized by factors other than the curvature energy: by dislocations emerging from the FCD's with  $e \neq 0$ , compression of layers and surface anchoring.

PACS number(s): 61.30.Eb, 61.30.Jf

### I. INTRODUCTION

Lamellar phases such as a smectic A liquid crystal with one-dimensional positional order often organize in distorted structures, with layers bent but still parallel to each other. The layers adopt the shape of Dupin cyclides, i.e., surfaces whose lines of curvature are circles. The reason is that the focal surfaces for Dupin cyclides degenerate into lines which reduces the singular energy. The defect lines are confocal pairs, usually an ellipse and hyperbola, around which the layers fold. The focal pairs serve as a frame of a focal conic domain (FCD) [1]. A particular case corresponding to an ellipse of zero eccentricity,  $e=0$ , is a pair of a circle and a straight line. Experimentally, one observes all the possible values of eccentricity in the range  $0 \leq e < 1$ . There is no universal explanation of this fact. The focal conics might also form around a pair of parabolas [2]; however, the parabolic FCD's are *not* the limiting case  $e=1$  of an ellipse-hyperbola FCD and have different elastic features not considered in this article.

Although the FCD's have been the subject of intensive studies for many years since the pioneering work by Friedel in 1922 [1], some basic features remain to be understood. Most notably, there is no analytical expression for the curvature energy of a FCD, except for the limiting case  $e \rightarrow 0$  [3]. Lifting this restriction is important in a number of problems, for example, in the description of tilt grain boundaries [4], nuclei of the lamellar phase appearing from an isotropic phase [5], oily streaks (set of dislocations decorated by FCD's) [6], and generally in any problem of filling space with curved lamellas. Both splay and saddle-splay energy terms should be included in the consideration, since the smectic layers in FCD's have a well-defined Gaussian curvature. FCD's in known thermotropic lamellar media manifest a negative Gaussian curvature; the corresponding domain is called a FCD of the first species, or FCD-I. FCD's of the second species (FCD-II's) with a positive Gaussian curvature reported recently for a lyotropic smectic phase [7] are rare. The energetics of FCD-II's is strongly influenced by the layers outside the domain that favor  $e=0$  [7]. This work presents an analytic expression for the curvature energy of

layers within a FCD-I of a negative Gaussian curvature and arbitrary eccentricity.

### II. STRUCTURE OF FCD-I

The theoretical framework of the analysis has been developed by Kléman [3]. In a FCD-I the layers fold around the conjugated ellipse  $E$  and one branch  $H$  of a hyperbola, in such a way that they are everywhere perpendicular to the straight lines joining any point  $M'$  on the ellipse to any point  $M''$  on the hyperbola, Fig. 1. Any point  $M$  on the line  $M'M''$  is the orthogonal intersection with this line of a uniquely defined surface (= layer)  $\Sigma_M$ , perpendicular everywhere to the two-parameter family of lines  $M'M''$ . All the parallel surfaces  $\Sigma_M$  orthogonal to  $M'M''$  have the same centers of curvature,  $M'$  and  $M''$ . The curvatures  $|\sigma'|=1/M'M$  or  $|\sigma''|=1/M''M$  become infinitely large when  $M$  approaches either  $M'$  or  $M''$ . Correspondingly,  $\Sigma_M$ 's are singular on  $M'$  and  $M''$ . Since the physical part of each layer lies between  $M'$  and  $M''$ , the Gaussian curvature is negative,  $\sigma'\sigma'' < 0$ .

Dupin cyclides in a FCD-I show up features varying with the position of  $M$  on the segment  $M'M''$ : either  $\Sigma_M$  ends on the ellipse on two point singularities (layers 1, Fig. 1), or  $\Sigma_M$  is free of singularities and looks similar to a deformed half-torus (layer 2), or it ends on the hyperbola, with two conical indentations (layers 3).

The equations for the confocal ellipse  $E$  and hyperbola  $H$ , located in two perpendicular planes, are

$$z=0, \quad \frac{x^2}{a^2} + \frac{y^2}{b^2} = 1 \quad (E); \quad (1)$$

$$y=0, \quad \frac{x^2}{a^2-b^2} - \frac{z^2}{b^2} = 1 \quad (H);$$

$a$  and  $b$  are the major and the minor semiaxes of the ellipse, respectively. Let  $M'(x', y', 0)$  be a point on  $E$  and  $M''(x'', 0, z'')$  be a point on  $H$ , and let us parametrize the conics in the usual way [3]:

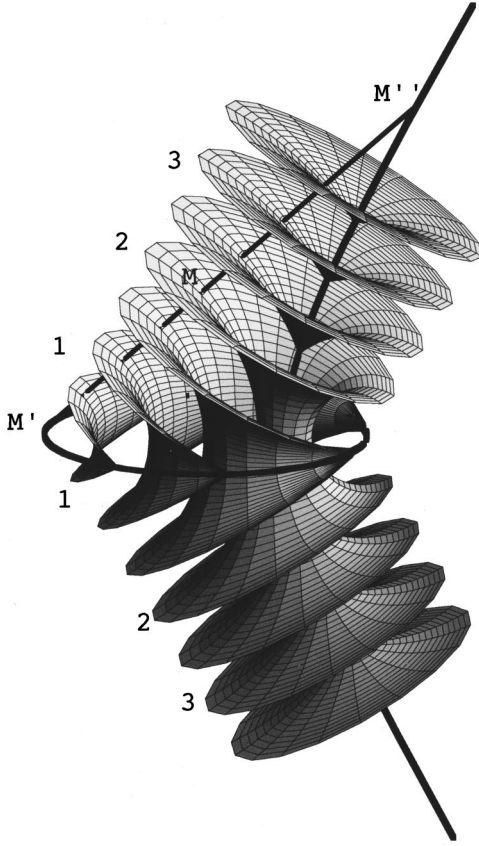


FIG. 1. General geometrical aspect of a FCD-I. The straight line  $M'M''$  is the direction perpendicular to the layer at point  $M$ ;  $M'$  and  $M''$  are points on the ellipse and the hyperbola, respectively.

$$M' \begin{cases} x' = a \cos u, \\ y' = b \sin u, \end{cases} \quad 0 \leq u < 2\pi, \quad (2)$$

$$M'' \begin{cases} x'' = c \cosh v, \\ z'' = b \sinh v, \end{cases} \quad -\infty \leq v \leq \infty,$$

where  $c^2 = a^2 - b^2$ . The principal curvatures of layers write

$$\sigma' = \frac{1}{c \cos u - r} < 0; \quad \sigma'' = \frac{1}{a \cosh v - r} > 0; \quad (3)$$

the choice of signs being arbitrary but consistent with  $\sigma' \sigma'' < 0$ ; the quantity  $r$  characterizes the position of point  $M$  and obeys the inequality

$$c \cos u < r < a \cosh v. \quad (4)$$

The whole set of  $r$  values for the *complete* FCD-I (shown in Fig. 1) is in the range  $[-c, +\infty[$ . The infinitesimal element of surface  $d\Sigma(r)$  of the  $\Sigma(r)$  cyclide is expressed through the principal curvatures as [3]

$$d\Sigma(r) = \frac{b^2 |\sigma' \sigma''|}{(\sigma' - \sigma'')^2} du dv. \quad (5)$$

### III. CURVATURE ENERGY

The curvature energy of the FCD-I is defined as the integral over the FCD-I's volume of the energy density  $f$  associ-

ated with the mean and Gaussian curvatures of layers:

$$f = \frac{1}{2} K (\sigma' + \sigma'')^2 + \bar{K} \sigma' \sigma''; \quad (6)$$

$K$  and  $\bar{K}$  are called the splay and the saddle-splay elastic constants. Note, however, that the splay term contains a saddle-splay contribution  $\sim \sigma' \sigma''$ . It is convenient to split the integral into two parts:

$$W = \int f d\Sigma dr = W_1 + W_2, \quad (7)$$

with

$$W_1 = -\frac{1}{2} K b^2 \int \sigma' \sigma'' du dv dr \quad (8)$$

$$= -\frac{1}{2} K (1 - e^2) a \int \frac{du dv d\rho}{(e \cos u - \rho)(\cosh v - \rho)},$$

$$W_2 = -(\bar{K} + 2K) b^2 \int \frac{\sigma'^2 \sigma''^2 du dv dr}{(\sigma' - \sigma'')^2} \quad (9)$$

$$= -\Lambda (1 - e^2) a \int \frac{du dv d\rho}{(\cosh v - e \cos u)^2},$$

and treat them apart. Here  $\Lambda = \bar{K} + 2K$ ,  $\rho = r/a$ . The Jacobian for the orthogonal coordinates  $(u, v, r)$  is the quantity  $b^2 |\sigma' \sigma''| / (\sigma' - \sigma'')^2$  in Eq. (5). Both  $K$  and  $\bar{K}$  terms contribute to the ‘‘topology,’’ since they appear in  $W_2$ , which is an integral of the Gauss-Bonnet type; the notation  $\Lambda = \bar{K} + 2K$  expresses this combined contribution.

#### A. $W_1$ term

The  $W_1$  term is singular near the ellipse and hyperbola, where  $r \rightarrow c \cos u$  and  $r \rightarrow a \cosh u$ . The phenomenological elastic theory should not be applied in these regions, and one has to restrict the region of integration by a cutoff length, called the core radius. Assume that the core radius does not depend on the layer (i.e., does not depend on  $r$ ):

$$r_{\text{cutoff}} = a \cosh v - r_c \quad \text{near the hyperbola,}$$

$$r_{\text{cutoff}} = c \cos u + r_c \quad \text{near the ellipse.}$$

The assumption greatly oversimplifies the situation: for example, it does not take into account that the layers that intersect the hyperbola far from the plane of the ellipse have practically no singularity. Furthermore, near the defect cores, the layers might suffer dilation, see Ref. [8] for a critical discussion.

Integrating Eq. (8) over  $\rho$  splits  $W_1$  into the singular  $W_{1\text{-sing}}$  and nonsingular  $W_{1\text{-nonsing}}$  parts:

$$W_{1\text{-sing}} = K a (1 - e^2) \ln \left( \frac{a}{r_c} \right) \int_{-\infty}^{\infty} dv \int_0^{2\pi} \frac{du}{\cosh v - e \cos u}, \quad (10)$$

$$W_{1\text{-nonsing}} = Ka(1-e^2) \int_{-\infty}^{\infty} d\nu \int_0^{2\pi} \frac{\ln(\cosh \nu - e \cos u) du}{\cosh \nu - e \cos u}. \quad (11)$$

It is easy to see (for example, by changing the variable,  $\cosh \nu \rightarrow 1/t$ ) that

$$\int_{-\infty}^{\infty} d\nu \int_0^{2\pi} \frac{du}{\cosh \nu - e \cos u} = 4\pi\mathcal{K}(e^2), \quad (12)$$

where

$$\mathcal{K}(x) = \int_0^1 \frac{dt}{\sqrt{(1-t^2)(1-x^2t^2)}}$$

is the complete elliptic integral of the first kind. Therefore, the singular term reads

$$W_{1\text{-sing}} = 4\pi Ka(1-e^2)\mathcal{K}(e^2)\ln \frac{a}{r_c}, \quad (13)$$

where  $r_c$  is typically of the order of the repeat distance of the layers. A specific core energy, that cannot be calculated with Eq. (6), should be added:  $W_{1\text{-sing}} \rightarrow W_{1\text{-sing}} + W_{\text{core}}$ , where  $W_{\text{core}}$  grows with the length of the defect. We omit  $W_{\text{core}}$ . In some cases, this omission can be justified by the fact that the parameter  $r_c$  can be renormalized to absorb  $W_{\text{core}}$  into  $W_{1\text{-sing}}$ .

The nonsingular part (11) of  $W_1$  is more difficult to evaluate. The problem is to find the integrals

$$I(e) = \int_{-\infty}^{\infty} d\nu \int_0^{2\pi} \frac{\ln(\cosh \nu - e \cos u)}{\cosh \nu - e \cos u} du \quad \text{and} \\ Q(\nu) = \int_0^{\pi} \frac{\ln(\cosh \nu - e \cos u)}{\cosh \nu - e \cos u} du, \quad (14)$$

that are related:

$$I(e) = 2 \int_{-\infty}^{\infty} Q(\nu) d\nu.$$

To evaluate  $Q(\nu)$ , let us denote  $A = \cosh \nu - e \cos u$ , and introduce  $\alpha = \exp(-\nu') < 1$ , where  $\cosh \nu' = \cosh \nu/e$ . Then  $A = \lambda(1 + \alpha^2 - 2\alpha \cos u)$ ,  $\lambda = e/2\alpha$ , and the integral takes a canonical form

$$Q = \int_0^{\pi} \frac{\ln \lambda}{\lambda(1 + \alpha^2 - 2\alpha \cos u)} du \\ + \int_0^{\pi} \frac{\ln(1 + \alpha^2 - 2\alpha \cos u)}{\lambda(1 + \alpha^2 - 2\alpha \cos u)} du \\ = \frac{\pi \ln \lambda}{\lambda(1 - \alpha^2)} + \frac{2\pi \ln(1 - \alpha^2)}{\lambda(1 - \alpha^2)}, \quad (15)$$

which can be checked by using MATHEMATICA 3.0; see also Ref. [9]. Returning to the original variable  $\nu$  in  $Q(\nu)$ , one writes  $I(e)$  as

$$I(e) = 8\pi \int_{-\infty}^{\infty} \frac{\ln \sqrt{\cosh^2 \nu - e^2}}{\sqrt{\cosh^2 \nu - e^2}} d\nu \\ + 4\pi \int_{-\infty}^{\infty} \frac{d\nu}{\sqrt{\cosh^2 \nu - e^2}} \ln \frac{2}{\cosh \nu + \sqrt{\cosh^2 \nu - e^2}} \\ = 8\pi I_1(e) + 4\pi I_2(e). \quad (16)$$

The first integral  $I_1(e)$  above is calculated by making the following change of the variable:

$$\frac{\cosh^2 \nu - e^2}{1 - e^2} = \frac{1}{\cos^2 x},$$

where  $0 < x < \pi/2$  when  $0 < u < \infty$ . Notice that this change of variable is not valid for  $e = 1$ . Then

$$I_1(e) = \int_0^{\pi/2} dx \frac{\ln(\sqrt{1-e^2}/\cos x)}{\sqrt{1-e^2} \sin^2 x} \\ = \mathcal{K}(e^2) \left[ \frac{\ln e}{2} + \frac{\ln(1-e^2)}{4} \right] + \frac{\pi}{4} \mathcal{K}(1-e^2). \quad (17)$$

To reduce the second integral  $I_2(e)$  in Eq. (16) to the table form, it suffices to change the variable as  $\cosh \nu = 1/t$ :

$$I_2(e) = \int_0^1 \ln \left( \frac{2t}{1 + \sqrt{1-e^2t^2}} \right) \frac{dt}{\sqrt{1-e^2t^2} \sqrt{1-t^2}} \\ = \mathcal{K}(e^2) \ln \frac{2}{e} - \frac{\pi}{2} \mathcal{K}(1-e^2). \quad (18)$$

Collecting the terms of the sum  $I(e) = 8\pi I_1(e) + 4\pi I_2(e)$ , one arrives at

$$W_{1\text{-nonsing}} = 4\pi Ka(1-e^2)\mathcal{K}(e^2)\ln(2\sqrt{1-e^2}). \quad (19)$$

### B. $W_2$ term

The  $W_2$  term (9) is integrated by employing Eq. (12):

$$W_2 = -4\pi\Lambda a(1-e^2)\mathcal{K}(e^2). \quad (20)$$

$W_2$  is negative when  $\Lambda$  is positive, a fact which is always insured if  $\bar{K} > -2K$ . Note that for the free energy density (6) to be positive definite for the lamellar phase,  $\bar{K}$  must be within the range  $-2K < \bar{K} \leq 0$ , which also means  $0 < \Lambda \leq 2K$  ( $K$  is always positive).

### C. Total curvature energy

The final expression for the total curvature energy  $W = W_{1\text{-nonsing}} + W_{1\text{-sing}} + W_2$ , valid for an arbitrary eccentricity  $0 \leq e < 1$ , adopts a very compact form:

$$W = 4\pi a(1-e^2)\mathcal{K}(e^2) \left[ K \ln \frac{2a\sqrt{1-e^2}}{r_c} - \Lambda \right]; \quad (21)$$

notice that  $a\sqrt{1-e^2} = b$ , where  $b$  is the minor semiaxis. For  $e = 0$ , Eq. (21) reproduces the known result [3,6]

$$W_0 = 2\pi^2 a \left[ K \ln \frac{2a}{r_c} - \Lambda \right]. \quad (22)$$

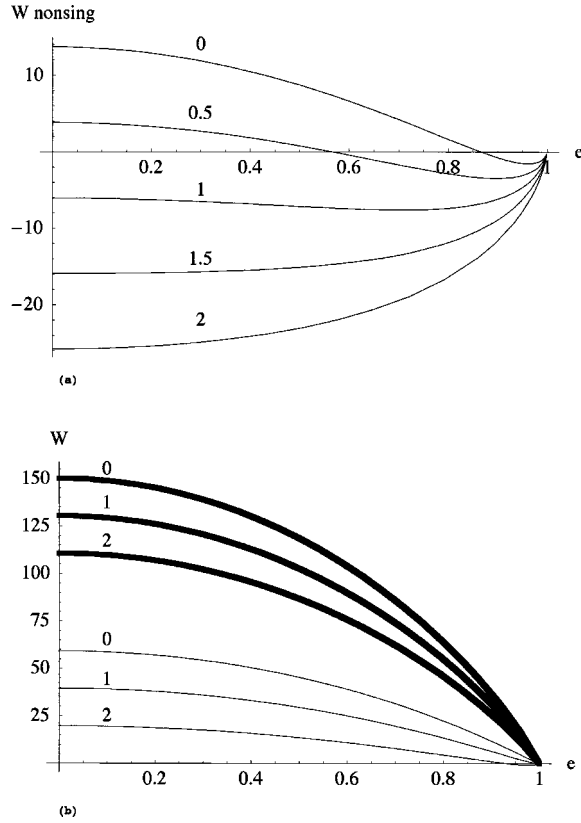


FIG. 2. Energies of FCD-I's vs eccentricity  $e$  for different values of the elastic parameter  $\Lambda/K$  (indicated by numbers above the curves); dimensionless units with  $K=1$  and a fixed major semiaxis  $a=1$ . (a) Nonsingular terms  $W_{\text{nonsing}} = W_{1\text{-nonsing}} + W_2$  vs  $e$ . (b) Total energy  $W = W_{1\text{-nonsing}} + W_{1\text{-sing}} + W_2$  vs  $e$  for FCD-I's of a large (thick lines,  $a/r_c = 1000$ ) and a small size (thin lines,  $a/r_c = 10$ ).

When  $\Lambda/K = \ln 2 \approx 0.693$ , the energy  $W_0$  reduces to its singular term.

#### IV. DISCUSSION

The expression (21) is the curvature energy of a FCD-I with an arbitrary eccentricity we have been looking for. Its validity is confirmed by numerical integration of the energy density (6) over the FCD-I's volume. The analytical form (21) allows one to trace the role of different parameters, for example, to find how the curvature energy depends on  $\bar{K}$  and  $e$  when the major semiaxis of the ellipse is fixed,  $a = \text{const}$ , Fig. 2.

The dependence of the curvature energies (21) and (22) on the saddle-splay elastic constant is obvious: the larger  $\bar{K}$ , the smaller is the energy; the reason is simply the negative sign of the Gaussian curvature of Dupin cyclides in a FCD-I. A further remark concerns the sum of the two nonsingular terms  $W_{1\text{-nonsing}} + W_2$  in  $W$  at  $a = \text{const}$ . When  $\Lambda$  increases, the coordinate of the minimum of the sum shifts from  $e \rightarrow 1$  to  $e \rightarrow 0$ , Fig. 2. The tendency of  $W_{1\text{-nonsing}} + W_2$  to reach a minimum at small eccentricity  $e \rightarrow 0$  is, of course, in competition with the increase of  $W_{1\text{-sing}}$  at  $e \rightarrow 0$ . Thus the minimum of curvature energy can be achieved at  $e$  somewhat different from 1 only when the domains are extremely small,  $a/r_c \sim 10$ , and when the saddle-splay constant is close to its upper limit  $\bar{K} = 0$ , set by the requirement of positive definite

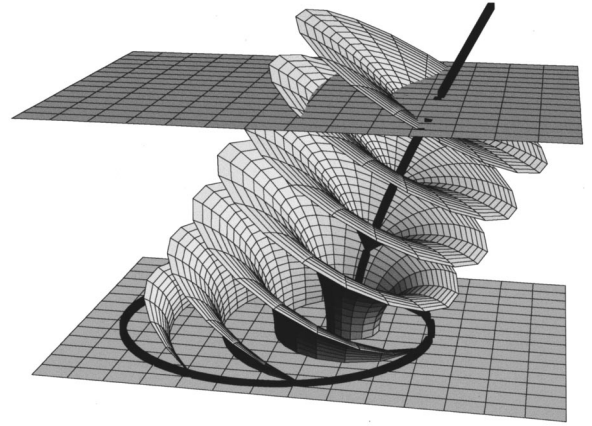


FIG. 3. FCD-I confined between two parallel plates in a flat cell. The smectic layers are perpendicular to the bottom plate and tilted at the top plate. The configuration of layers causes anchoring energy penalties for both polar (out-of-the-plane) and azimuthal (in-plane) angles.

value of  $f$  in Eq. (6), see Fig. 2(b). Generally, for a reasonably large domain,  $a/r_c > 10$ , the curvature energy becomes minimum only at  $e \rightarrow 1$ , Fig. 2(b), a fact that has been already foreseen on the basis of numerical calculations [3]. However, it would be a mistake to conclude that a FCD-I tends to increase its eccentricity as much as possible on the ground of Eq. (21). The reason is that in real samples the FCD's are rarely isolated; their elastic energy is only a part of the total energy that includes the energy of surface anchoring, dislocations, layers compressions, etc., as discussed below.

First, note that the plots in Fig. 2 correspond to a fixed major semiaxis,  $a = \text{const}$ . The volumes of FCD-I's with identical  $a$ 's but different  $e$ 's are obviously different; they scale as  $\sim a^3(1 - e^2) = ab^2$ . When  $a = \text{const}$ , an increase of  $e$  means a decrease of the minor semiaxis  $b$ . Thus the curvature energies of two FCD's with different  $e$ 's should be compared under additional geometrical constraints. These constraints in concrete experimental situations involve the finite size of the system and thus require to consider also the surface anchoring energies that have been shown to be rather large in smectic phases [10,11]. The effect of confinement is illustrated in Fig. 3. The elliptical base of a FCD-I is located at the bottom plate of a flat sample, which can be provoked by a tangential anchoring at this plate (the molecules are parallel and the layers are perpendicular to the plate, Fig. 3). At the top plate, the layers are tilted. The tilt angle changes from point to point, which necessarily results in an anchoring energy penalty associated with the polar (out-of-plane) angles [11]. Furthermore, if the bounding plates are not isotropic, FCD-I geometry provokes not only the polar but also an azimuthal (in-plane) anchoring energy penalty: in Fig. 3, the curved layers deviate from any of the possible straight lines drawn in the plane of the cell. Both polar and azimuthal anchoring energies depend on  $e$  and thus influence any minimization problem for a confined geometry.

The second reason that limits  $e$  relates to the fact that layers inside the FCD-I's should match the layers outside the domains. Because of their peculiar shape, FCD-I's cannot fill a bounded piece of space as isolated objects. They have to be embedded in the surrounding matrix of smectic layers, that might be flat or curved. When the FCD-I of a small eccen-

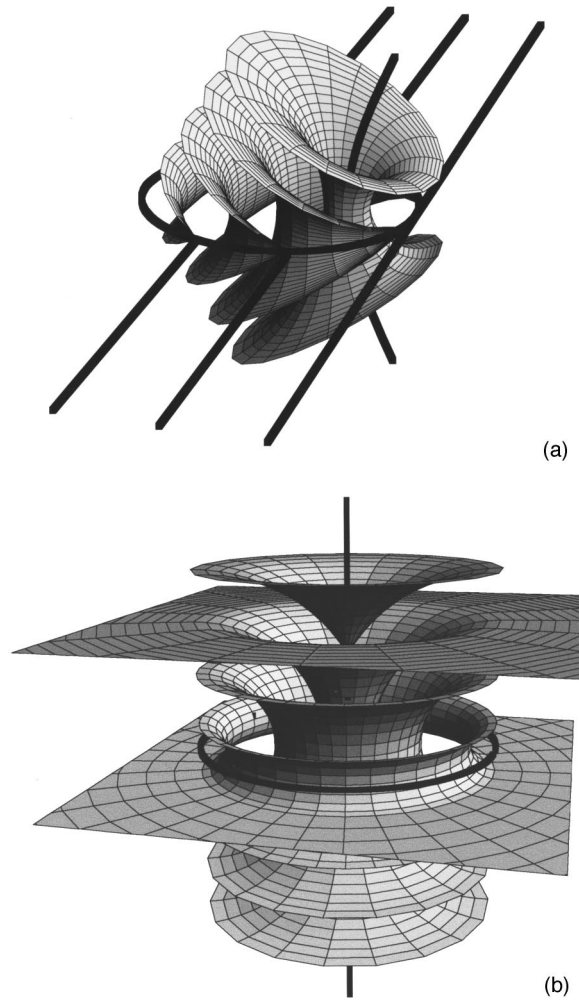


FIG. 4. FCD-I of nonzero (a) and zero eccentricity (b). Nonzero eccentricity is the cause of the appearance of dislocations [shown by thick horizontal lines in (a)] outside the FCD-I. In contrast, the FCD-I with  $e=0$  can be smoothly embedded into a system of flat parallel layers; two such smoothly matching flat layers outside the FCD-I are shown in (b).

tricity  $e > 0$  is embedded into a system of flat layers, the tilt of smectic layers *inside* the FCD-I (with respect to the horizontal plane) requires a matching dislocation set *outside* the FCD-I [12,6]. These dislocations run along the direction of the minor semiaxis of ellipse, Fig. 4(a). The total Burgers vector  $b_e$  of the dislocation set is directly related to the eccentricity and the size of ellipse [6]:  $b_e = 2ae$ . Each disloca-

tion carries an elastic energy proportional to the Burgers vector [13],  $\sim \sqrt{BK}b_e$  (per unit length); here  $B$  is the compression modulus. Thus although the trend  $e \rightarrow 1$  is favored by the curvature of layers *inside* the FCD-I, an opposite trend  $e \rightarrow 0$  is favored by the line tension  $\sim \sqrt{BK}ae$  of dislocations *outside* the FCD-I. It is only when the eccentricity is zero that the dislocations do not appear; a toroidal FCD-I with  $e=0$  can be smoothly embedded into the system of flat and parallel smectic layers, Fig. 4(b). A more detailed analysis of matching between the layers inside and outside the FCD-I's (that includes the case when the outside layers are curved) is given in Ref. [4]. Note also that the compression energy density  $B\varepsilon^2/2$  results in additional  $e$ -dependent energy terms, important near the cores of confocal pairs, as discussed by Fournier [8].

Overall, the problem of finding an equilibrium  $e$  requires consideration of factors additional to the curvature energy, such as dislocations, layers' compressibility and surface anchoring phenomena. One should bear this in mind when analyzing different results on FCD's energies. For example, the estimation [6] of the saddle-splay elastic constant  $\bar{K}$  from the features of FCD-I's in oily streaks has been possible to carry out only for  $B=0$ . As explained by Boltenhagen *et al.* [6], the model with  $B=0$  leads to a large positive  $\bar{K}$  which is thus only an indicator that the system under investigation favors deformations with a negative Gaussian curvature rather than with a positive Gaussian curvature. Lifting the restriction  $B=0$  contributes to the decrease of  $e$  and thus decrease the estimated  $\bar{K}$  due to the dislocations and compressibility effects discussed above; the exact analytical analysis of the oily streaks for  $B \neq 0$  has not yet been done.

Finally, note that in some instances, the eccentricity  $e$  is not a parameter of energy minimization at all. An array of FCD-I's forming a grain boundary [4] is a good example of a situation where the true minimizer is the size rather than the eccentricity: the eccentricity is fixed by the angle  $\omega$  of misalignment of layers in two adjacent monodomains,  $e(\omega) = |\sin(\omega/2)|$ . The result (21) allows one to calculate the energy of such a grain boundary and to find the characteristic size of the FCD's in it [4].

#### ACKNOWLEDGMENTS

The work was supported by the NSF U.S.–France Cooperative Scientific Program, Grant No. INT-9726802 and by NSF STC ALCOM under Grant No. DMR89-20147. All figures in this article were generated using MATHEMATICA 3.0.

[1] G. Friedel, *Ann. Phys. (Paris)* **18**, 273 (1922).  
 [2] C. S. Rosenblatt, R. Pindak, N. A. Clark, and R. B. Meyer, *J. Phys. (France)* **38**, 1105 (1977).  
 [3] M. Kleman, *J. Phys. (France)* **38**, 1511 (1977).  
 [4] M. Kleman and O. D. Lavrentovich, *Eur. Phys. J. B* (to be published).  
 [5] J. B. Fournier and G. Durand, *J. Phys. II* **1**, 845 (1991).  
 [6] P. Boltenhagen, O. D. Lavrentovich, and M. Kléman, *J. Phys. II* **1**, 1233 (1991).

[7] Ph. Boltenhagen, O. D. Lavrentovich, and M. Kleman, *Phys. Rev. A* **46**, R1743 (1992).  
 [8] J. B. Fournier, *Phys. Rev. E* **50**, 2868 (1994).  
 [9] A. P. Prudnikov, Yu. A. Brychkov, and O. I. Marichev, *Integraly i Ryady* (Nauka, Moscow 1981), p. 800 (in Russian).  
 [10] G. Durand, *Liq. Cryst.* **14**, 159 (1993).  
 [11] Z. Li and O. D. Lavrentovich, *Phys. Rev. Lett.* **73**, 280 (1994).  
 [12] J. Friedel and M. Kleman, *J. Phys. (France)* **30**, C4:43 (1969).  
 [13] M. Kleman, *Points, Lines and Walls* (Wiley, New York, 1982).